https://doi.org/10.1016/j.nanoen.2019.01.056

Towards Truly Wearable Energy Harvesters with Full Structural Integrity of Fiber Materials

Jianliang Gong, Bingang Xu,* Xiaoyang Guan, Yuejiao Chen, Shengyan Li, Jie Feng

Nanotechnology Center, Institute of Textiles and Clothing, The Hong Kong Polytechnic University, Hung Hom, Kowloon, Hong Kong, P. R. China

*To whom correspondence should be addressed.

E-mail: tcxubg@polyu.edu.hk; Tel: +852-2766 4544

ACKNOWLEDGMENTS

This work reported in this paper is supported by the Hong Kong Polytechnic University (Project No. 1-YW1B, G-UACC, and G-YBV2). The authors would also thank Dr. Su Liu, Ms. Suki Siu and Ms. Bingyu Liu for their kind assistances on computerized knitting and applications of A-TEHs for harvesting mechanical energy.

Abstract

Through full flexible realization of a new energy harvesting mode using only common fiber materials as active components by adopting a computerized knitting programme strategy, herein we developed a new kind of all-textile energy harvesters (A-TEHs) with a three-dimensional fabric structural integrity that can harvest and convert mechanical energy to electricity directly. The electric performance of obtained A-TEHs working at a single-electrode mode was extraordinary, which can generate a maximum power density of 1768.2 mW m^{-2} by 1200 N at a matched resistance load of 50 MΩ, and directly light up over 320 LEDs instantaneously by a single impact with an effective area of only 56.7 cm^2. When A-TEH was used to charge a 200 μF commercial capacitor storage device with a bridge rectifier, its charging capacity increased with the triggering force, ranging from 6.7 mV s^{-1} at 100 N to 11.3 mV s^{-1} at 1400 N. Benefiting from the full structural integrity of fiber materials, A-TEHs, for the first time, truly realized the excellent textile properties that all wearable electronics try to achieve, including safety, lightweight, comfort, breathability, washability, and unique advantage of tailorability, leading to a kind of truly wearable energy harvesters with versatile product designability.

Keywords: Energy harvester; Fabric structural integrity; Fiber assemblies; Full textile properties; True wearability

1. Introduction

Development of wearable electronics that can be truly and directly worn on human body with desired functional performance, uncompromised safety and good wearing comfort, or what is called truly wearable electronics, is a common and ultimate goal of scholars and professionals worldwide from a broad range of disciplines of physics, chemistry, materials, electrical and electronics, etc. Over the past decade, progressive milestones have been witnessed in this promising and fast-growing area with notable examples of wearable transistors/logic circuits,[1-3] multiplex sensor arrays,[4] thermal management systems,[5,6] and energy harvesting/ storage devices[7-14] by structural engineering of rigid electronic circuits and devices as flexible/stretchable components. It is encouraging to see increasing functional performance has been achieved, but most wearable electronics are either in form of films or use textiles as a substrate for embedding with electronic devices/chemical components, and development of truly wearable electronics with an integrity of functionality, safety, comfortability remains a global challenge both academically and industrially still. To be truly wearable, the developed wearable electronics should meet the following key requirements: (1) excellent electrical/electronic properties with desired functional performance; (2) good wearing comfort so that it is more realistic for people to wear in their daily lives; (3) both constituent materials and functional properties must be safe for people under various conditions and environment; (4) durable

enough to withstand the severe wearing conditions for a long period of time; (5) easy to care like washing-drying operation without degrading its electrical performance; and (6) can be efficiently fabricated and easily scaled-up for a wide and versatile application.

Electronic devices cannot work without electric power supply. To obtain truly wearable electronics, electric power sources must be firstly developed and endowed with safe, washable, durable, flexible, miniature, scalable, easy-care and lightweight characteristics. So far, however, the electric power for wearable and portable electronics still overwhelmingly rely on environmentally-unfriendly batteries based on non-renewable sources. An alternative is to develop energy harvesters capable of converting ambient solar, thermal or mechanical energy into electricity renewably and sustainably. They are idea power sources to replace traditional batteries for directly driving huge number of milli-/micro-watt electronic devices (the power of which still has a continuously decreasing trend). The normal and high-performed operations of conventional energy harvesters (often in solid and bulky appearance), however, require limited functional materials with special photovoltaic, pyroelectric, piezoelectric or excellent triboelectric properties.[8, 15-17] And their functional performance often requires to be activated and be conserved under rigorous processing and/or packaging conditions such as dust-free conditions, thermal/vacuum annealing, and high voltage polarization. These limitations and disadvantages result in the uncompetitive cost of energy harvesters in large scale production for generating electric power and will inevitably return to the depletion dilemma of non-renewable

functional materials in the long term. Moreover, the bulky and rigid nature of functional materials is also an insurmountable obstacle to develop energy harvesters for true and full integration with electronic devices, particularly for flexible and wearable electronics. Therefore, both traditional batteries and conventional energy harvesters are still far from being able to meet the truly wearable requirements of power sources.

Triboelectric nanogenerator (TENG) is a novel kind of energy harvesters recently developed based on conjunctive use of contact electrification and electrostatic induction, which can directly convert mechanical energy into electricity through simple contact and separation of two materials with excellent but opposite triboelectric properties.[18-21] The assembly of TENGs reported over the past several years can be briefly generalized into two main keys: (1) design of revertible structures based on two different kinds of triboelectric materials for generation of immobile triboelectric charges by repetitive contact-separation process and (2) incorporation of electrodes close to noncontact surface of triboelectric materials for electrostatic induction of mobile electrons. A common strategy is to introduce an elastic sponge or spring between two polymer films adhering to a conductive layer laminated or coated on an additional substrate as supporting,[22-24] which often results in TENGs with solid and bulky structures. More recently, attempts were also made to endow TENGs with flexible and lightweight characteristics, such as directly replacing solid films with stretchable fabrics,[25] embedding conductive strips with insulating fabrics,[26] coating/growing nanomaterials (e.g. ZnO rods and graphene) on the outer

surface of fabrics,[27, 28] and simple weaving or knitting of a silicone rubber coated stainless steel/polyester fiber blended yarn by hands.[29, 30] These approaches are valuable and lead to a kind of fabric-like TENGs with promising textile-related applications. However, their electric output performance was usually not as good as those of solid TENGs. Moreover, the multistep assembling processes of TENGs generally include one or more manual tailor-made procedures. And fabric-like TENGs still cannot achieve a full and scalable integration of energy harvesters into true textiles, namely cannot fully meet the high and stringent requirements of truly wearable power sources and electronic devices.

Herein, we developed a new energy harvesting model with enhanced effects of contact electrification and electrostatic induction by doubling the contact and separation processes of triboelectric materials in a triggering cycle, and most significantly, realized it as a flexible and freestanding 3D fabric structural integrity directly with safe and common fiber materials by adopting a reliable textile engineering strategy. It leads to a novel kind of all-textile energy harvesters (A-TEHs) with full properties (such as excellent durability, washability, scalability and unique tailorability) of fabrics and excellent electric performance of energy harvesters, which fully meet the above-mentioned truly wearable requirements of electronics.

2. Results and Discussion

The simplified physical model (rigid-spring system) of our energy harvesters is illustrated in Fig. 1a, where a rigid conductive layer (CL) is suspended on a rigid

dielectric layer I (DL-I) with the support of springs. It works as a single-electrode mode by grounding CL (Fig. 1b), which is triggered by dielectric layer II (DL-II). Its operational principle is based on contact electrification effect coupling with electrostatic induction effect.[31-33] Fig. 1c illustrates the generation processes of electricity during a triggering cycle. Specifically, when DL-II impacts CL and DL-I repetitively, the transfer of electrons, ions and/or molecules is believed to occur between their contacting areas,[34-36] leading to the generation of opposite but equal triboelectric charges on DLs and CL macroscopically, respectively. If both DL-I and DL-II tend to be more negatively charged than CL, negative triboelectric charges will be formed on their surfaces, respectively. And owing to the excellent insulation properties of used dielectric materials, negative triboelectric charges can be assumed to distribute on the surface of dielectric layer uniformly at macro scale with negligible decay; while because of the single electrode by grounding, the generated triboelectric charges on CL can be regarded to be completely neutralized by electrons from the ground at a suitable separation distance (Fig. 1c-i). When the negatively charged DL-II starts to move toward CL, electrons will be driven through the load to the ground for induced formation of positive charges on CL (Fig. 1c-ii) to balance the negative triboelectric charges of DL-II, which contributes to a current flow from the conductive layer to the ground. After reaching CL, the negative triboelectric charges of DL-II will be balanced (Fig. 1c-iii). Then DL-II and CL will continuously move close to the negatively charged DL-I together for further induction of positive charges on conductive layer, which forms a current flow with the same direction (Fig. 1c-iv).

After close contact with CL-I, electrical equilibrium will reach (Fig. 1c-v). During the subsequent separating processes, CL will be recovered firstly (Fig. 1c-vi and vii), and then DL-II will leave CL (Fig. 1c-viii), and finally return to the initial state. The increasing distance will result in weakening the effect of electrostatic induction, so that electrons will flow back from ground to neutralize the positive charges on CL, which leads to form a current flow with opposite direction.

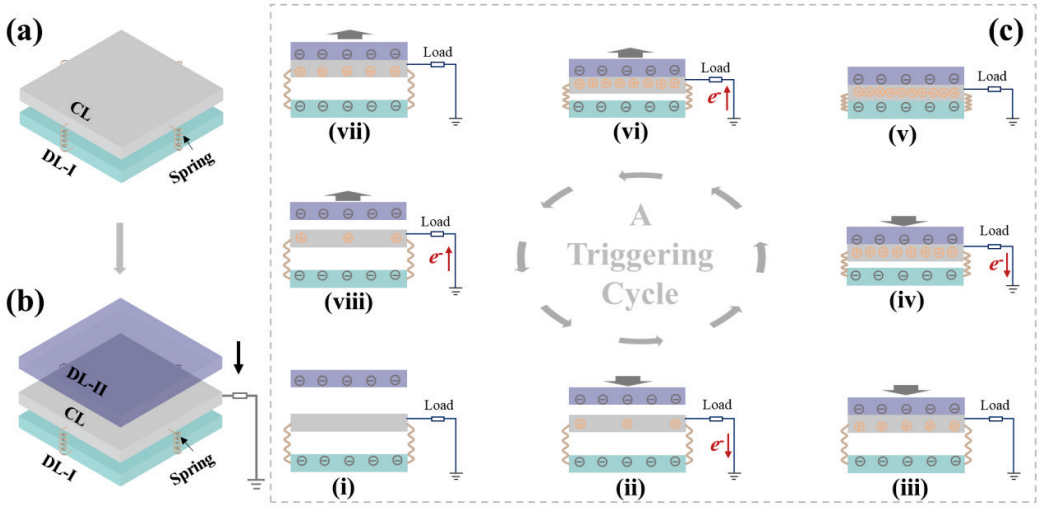

Figure 1 Schematics of (a) a new energy harvesting model (rigid-spring system) based on coupling effects of contact electrification and electrostatic induction, (b) its operational mode and (c) operational principle during a triggering cycle: (i) initial separation state among CL, DL-I and DL-II, (ii) DL-II contacting to CL, (iii) DL-II contacted with CL, (iv) DL-II and CL contacting to DL-I, (v) DL-II and CL contacted with DL-I, (vi) DL-II and CL leaving DL-I, (vii) CL recovered, (viii) DL-II continuously leaving conductive top layer, and finally back to the initial separation state

Comparing to conventional contact-separation modes with single separation/contact process in an impact cycle, one advantage of this new energy harvesting mode is to enhance both contact electrification and electrostatic induction effects of triboelectric materials by doubling their contact and separation processes in an impact cycle without the need of increasing the area sizes of devices. And the introduction of

springs between CL and DL-1 contributes to yielding resilience forces for instantaneous separation when external triggering forces on DL-II removed. When we used a copper sheet, two PDMS films to serve as CL, DL-I and DL-II, respectively, their repetitive contacting and separating processes will drive the electrons flowing forth and back across the external resistor load repetitively and lead to form an alternating voltage, as demonstrated in the insets of Fig. 2i. It also indicates that the new energy harvesting mode generates an electric signal with bimodal-peak characteristics, which can be clearly observed after magnification (Fig. 2i). This phenomenon is different from the simple electric signals generated by conventional contact-separation modes (Fig. S1). Assuming the resistor load is a pure resistance, the electric energy (E) generated by an impact is equal to the Joule heating and can be calculated based on time-integral of the output voltage signals with the following equation:

$$E=Q=\int_{t_1}^{t_2}\frac{U^2}{R}dt$$

where E is the electric energy generated by energy harvesters, Q is the Joule heating energy, U is the output voltage, R is the load resistance, and t_1 and t_2 represent the start time and end time of a single impact, respectively.

The calculated results based on experimental data demonstrated that our new energy harvesting model with bimodal peaks can generate approximately 84%-177% more electric power than the conventional models with simple peaks under the same triggering forces of 300 N-1000 N. The reasons of bimodal peaks can be ascribed to

the successive contact and separation of PDMS films with copper sheet twice during a triggering cycle, as demonstrated in Fig. 2a-h. They are generally correspondent to the electric signals marked in Fig. 2i. The insets of Fig. 2a-h indicate that the electricity generation processes of the new energy harvesting mode illustrated in Fig. 1c show good consistency with experimental results. This phenomenon of new energy harvesting mode with double contact and separation processes can be more clearly observed by the slow-motion video in real time and well differentiated with that of conventional contact-separation modes (Movie S1).

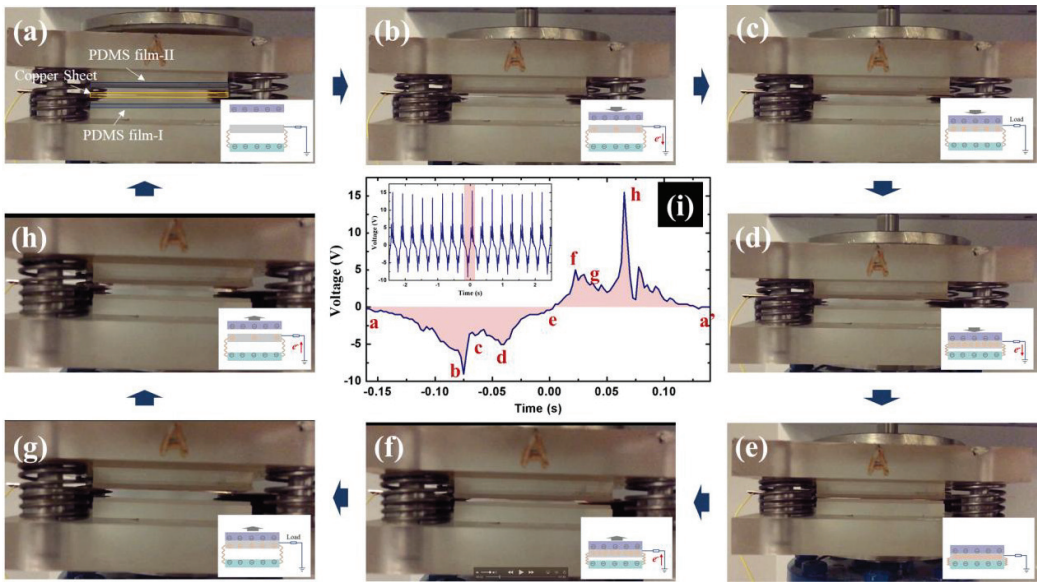

Figure 2 Experimental simulation of new energy harvesting model and its different instantaneous states during a triggering cycle: (a) initial separation state among copper sheet, PDMS film-I and PDMS film-II, (b) PDMS film-II contacting to copper sheet, (c) PDMS film-II contacted with copper sheet, (d) PDMS film-II and copper sheet contacting to copper sheet, (e) PDMS film-II and copper sheet contacted with PDMS film-II, (f) PDMS film-II and copper sheet leaving copper sheet, (g) copper sheet recovered, (h) PDMS film-II continuously leaving copper sheet, and finally back to the initial separation state. (i) The magnified electric signal of a triggering cycle generated by this energy harvesting model. Its inset shows the typical electric signals generated *via* repetitive triggering forces. The copper sheet and two PDMS films (I and II) were served as CL, DL-I and DL-II, respectively. The marked letters generally show their electric signals triggered at different moments (correspondent to

(a)-(e)), which show good consistency with the electricity generation processes of the new energy harvesting mode illustrated in Fig. 1c

Fig. 3a illustrates the corresponding flexible-body system of the new energy harvesting model. The CL, springs and DL-I of rigid model are designed and constructed as a full flexible structural integrity with one flexible conductive layer, one layer consisted of flexible dielectric beams and one flexible dielectric layer, respectively. It also works as a single-electrode mode by grounding the conductive layer (Fig. 3b), which can be triggered by any external active objects with a dielectric surface (equivalent to DL-II). The conductive top layer of this flexible energy harvesting model plays dual roles of triboelectric surface and electrode, and the dielectric bottom layer acts as another triboelectric surface and nonconductive substrate to prevent electrons randomly dissipating into ground, while dielectric middle layer of beam assemblies provides rebound resilience like springs.

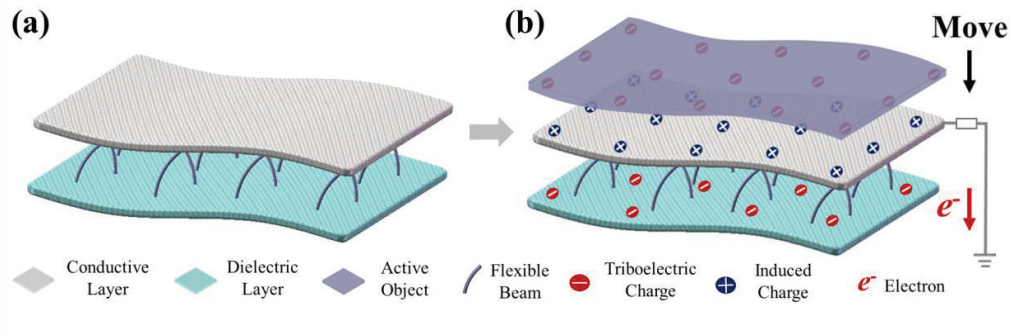

Figure 3 Schematics of (a) the corresponding flexible-body system of new energy harvesting model, (b) its operational principles for converting mechanical energy to electricity triggered by an active object.

To realize the full flexibility of energy harvesting model, we adopted a computerized knitting strategy for its fabrication with three sets of fibers using computer programming. As illustrated in Fig. 4a, one set of conductive fibers with positively

charged tendency (e.g. conductive silver-plated nylon fibers) and one set of dielectric fibers with negatively charged tendency (e.g. polyacrylonitrile (PAN) fibers) are used to directly knit the conductive top layer and dielectric bottom layer, respectively. To minimize the disturbance of other materials on contact electrification between conductive top layer and dielectric bottom layer, the triboelectric property of the third fiber for dielectric middle beam layer can be neutral (e.g. cotton)[37, 38] or identical with that for bottom layer. The third set of fibers is alternatively knitted with a defined sequence to link the conductive top layer and dielectric bottom layer as a structural integrity, meanwhile to construct hollow spaces between them. This textile engineering strategy leads to a kind of truly fabric A-TEHs with all conductive top layer, dielectric middle layer and dielectric bottom layer fully integrated with elaborate knit loop structures (Fig. 4b). Fig. 4c is a photograph of a 20 cm x 20 cm A-TEH knitted with commercially available silver-plated nylon, PAN and cotton fibers on a computerized flat knitting machine with programming. The typical microstructures of its conductive top layer, dielectric bottom layer, and dielectric middle layer are shown in Fig. 4d, e, and f, respectively. Fig. 4f indicates that the distance between the conductive top layer and dielectric bottom layer is about 1 mm. It is obvious that A-TEHs elaborately realize the main components of TENGs, namely triboelectric materials, elastic spacer/springs and conductive electrodes, as a flexible and full fabric structural integrity. Comparing to most reported TENGs, the A-TEH is ultrathin (<5 mm), light-weight (<0.08 g cm^{-2}), and flexible for scrolling (Fig. 4g), folding (Fig. 4h) and kneading (Fig. 4i). Owing to special space structure, it is also

wrinkle-resistant. As shown in Fig. 4i, A-TEH after heavily kneading can be easily recovered by simply releasing and smoothing with hands (For more details, see Movie S2). Moreover, the size of A-TEHs can be directly, economically and rapidly scalable with computerized knitting with programming (Fig. 4j) (For more details, see Movie S3).

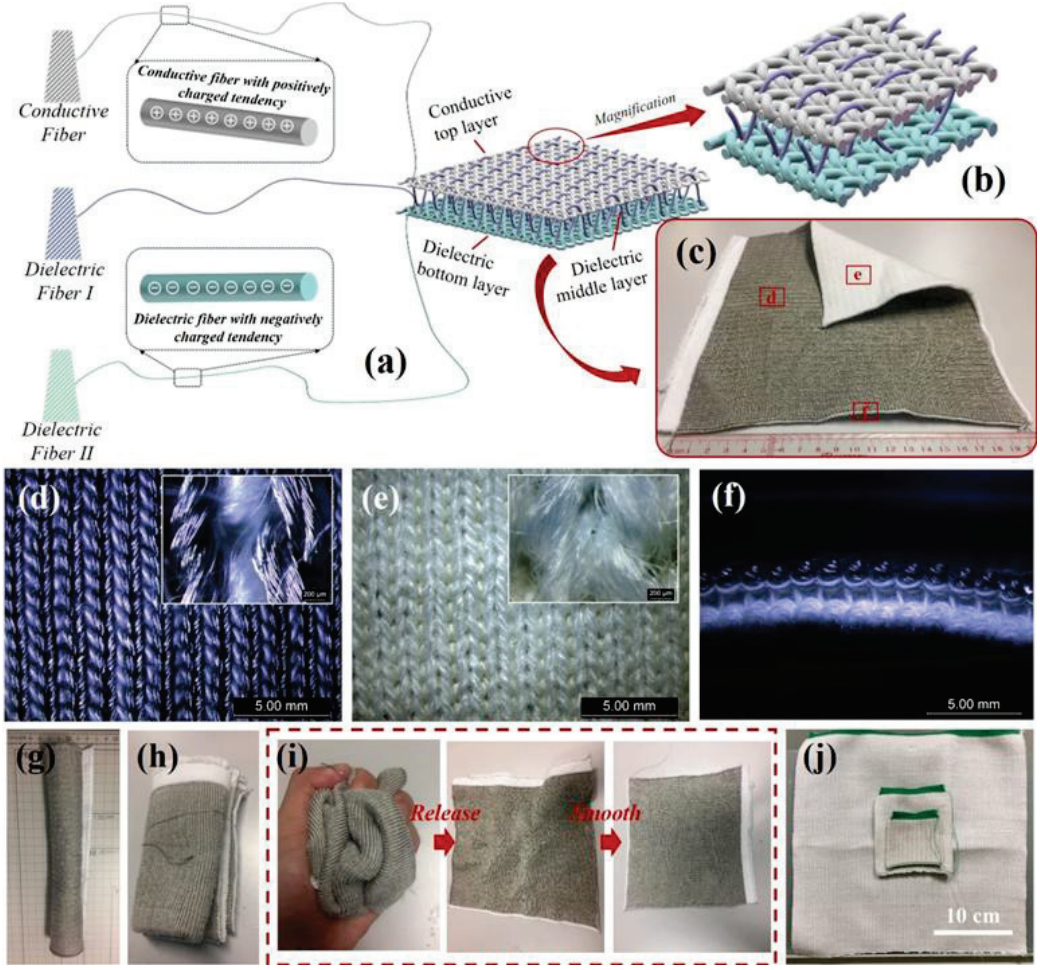

Figure 4 (a) Schematic illustration of realizing the energy harvesting mode as a 3D full fabric structural integrity using all fiber materials by computerized knitting programming and (b) its resultant A-TEHs with loop structures. (c) digital photograph of a typical A-TEH with 20 x 20 cm, and its optical images of (d) conductive top layer, (e) dielectric bottom layer, and (f) dielectric middle layer. The insets are magnified views of knit loops. (g)-(i) super flexibility of A-TEH and its wrinkle-resistant property, (j) different sizes of A-TEHs knitted on a computerized equipment with programming

The obtained A-TEHs can generate electric power directly and easily by the flap of any objects with a dielectric surface. To evaluate the electric performance quantitatively, a cyclic impact force by an active object, a polydimethylsiloxane (PDMS) film, was repetitively applied on the conductive surface of A-TEH with a contacting diameter of 8.5 cm, as illustrated in Fig. 5a. The generated voltages across an equivalent pure resistance load of 8 MΩ were firstly monitored and measured, displaying an alternating electric signal with an identical frequency of applied force (Fig. 5b). Each impact cycle involving a contact and separation led to a pair of positive bimodal peak and negative bimodal peak with approximate symmetry (Fig. 5c), which were sequentially generated during the contacting processes of conductive top layer with active object (C1) and dielectric bottom layer (C2), and the separating processes of conductive top layer with dielectric bottom layer (S2) and active object (S1), respectively. These electricity generation processes well coincide to those of energy harvesting model based on rigid-spring system above. Fig. 5d shows that the electric power of A-TEH is scalable, which is increased with the increase of applied impact force. This increasing trend can be obviously observed by its maximum output voltages and current densities shown in Fig. 5e. Based on $P=U^2/(RA)$ (P: output power, U: output voltage, R: load resistance, A: contacting area), the maximum output power of A-TEH under different impact forces was obtained, which increases from 125.9 mW m^{-2} to 825.4 mW m^{-2} over the applied force range of 100 N to 1400 N. The fitting results in Fig. 5f indicated that the output power density of A-TEH displays a linear increase trend with applied impact

force, which can be modelled by P= 82.724 + 0.482x (where P is output power and x is the applied impact force, Adj. R-square is 0.974). The influence of load resistance on the electric performance of A-TEH was also investigated by fixing the applied force at 1200 N. As shown in Fig. 5g, the current density generally decreased with the load resistance, while the output voltage across the resistance load exhibited an increase trend. Correspondingly, the power density of A-TEHs firstly increased at the low resistance region and then decreased with the increase of load resistance (Fig. 5h). When the resistance of load is 50 MΩ, a maximum value of 1768.2 mW m^{-2} can be obtained. These results show that our A-TEHs using only common fiber materials can generate electric power much more efficiently than alternative energy harvesters based on functional materials with special piezoelectric property, which usually create small electric signals (mV-V voltage output or nA-mA current range).[8, 14]

Compared with fabric-like arc-shaped[25] and PDMS coated[29,30] triboelectric nanogenerators with multistep and complicated manual assembling procedures, our A-TEHs with safe fiber materials by directly computerized knitting, also show a significantly higher output power than ~6 mW m^{-2} [25], ~52 and 34 mW m^{-2} [29,30] at the same conditions. The excellent electric performance of our novel A-TEHs can be attributed to the greatly enhanced effects of both contact electrification and electrostatic induction because of (i) doubled contact and separation processes based on innovative structural design of triboelectric materials, (ii) enhanced charge collection owing to the intimate contact between flexible fiber materials, and (iii)

increased effective contact areas caused by the uniform transfer of impact force across the fabric layers. Moreover, benefiting from the integration of all fiber materials as a 3D flexible fabric structural integrity by knitting, this novel kind of A-TEHs is highly durable for electric power generation. No electric performance degradation or device damage was observed when using an impacting force over 1000 N to repetitively strike the same region for 100,000 times (Fig.5i). And besides applied impact force, the electric performance of our A-TEHs on harvesting mechanical energy can also be scalable by increasing contacting area and impact frequency (Fig. S2). A-TEHs can harvest the mechanical energy triggered in a broad frequency range and the triggering frequency can be as low as 0.1 Hz.

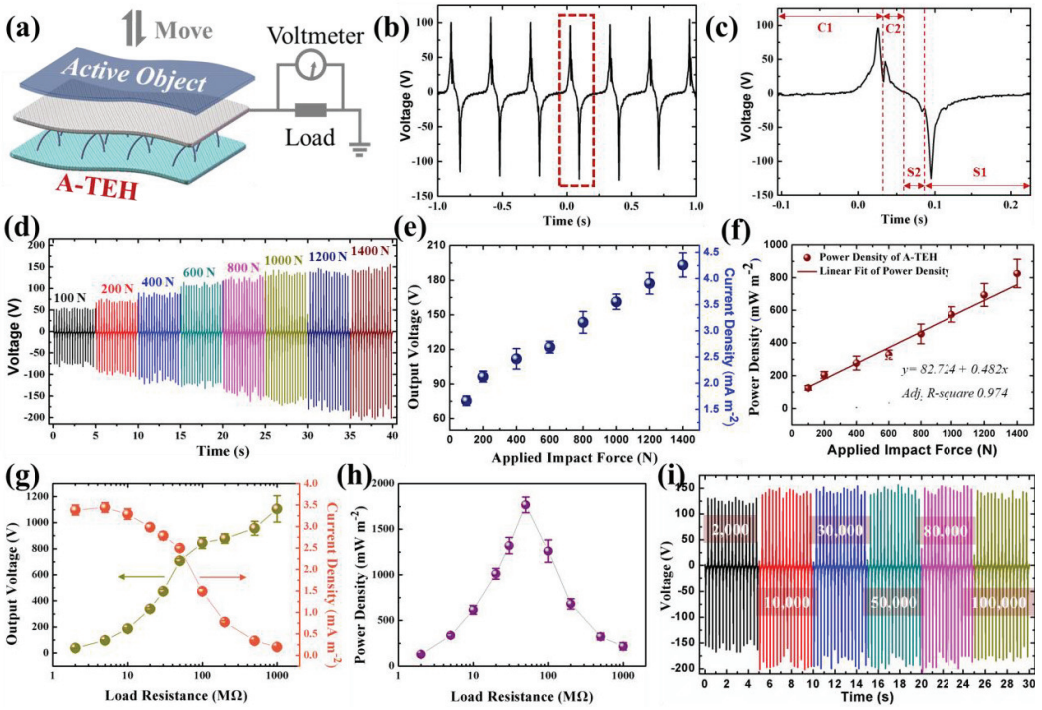

Figure 5 Electric power performance of A-TEHs for harvesting mechanical energy: (a) schematic diagram of evaluating A-TEHs with a single-electrode circuit, (b) typical voltage signals triggered by a PDMS film at 500 N and (c) its magnified signal generated by one impact cycle; (d) the output voltages under different applied impact forces at 3.3 Hz and their (e) maximum output voltages and current densities, and (f)

power densities; the dependence of (g) output voltage, current density and (h) power density on load resistance, (i) electric performance durability of A-TEHs

The electric power generated by our A-TEHs can be directly used to drive consumer electronics, such as commercial LEDs. Fig. 6a shows different LEDs were connected to A-TEH in series to form various patterns. All of them were easily lighted up by impacting A-TEHs. More encouragingly, our A-TEHs can light up over 320 LEDs instantaneously by a single impact on a 10 cm x 10 cm A-TEH sample with an actual contacting area of 56.7 cm^2 (i.e. a diameter of 8.5 cm, Fig. 6b and see Movie S4). The generated electric power can also be stored in energy storage devices (such as capacitors) after rectifying. And through monitoring the charging voltages, the true capacity of A-TEH can be evaluated more accurately. A 200 μF commercial capacitor was connected to the A-TEH with a bridge rectifier. The used rectifying circuit was illustrated in the inset of Fig. 6c, which can transform the alternating voltage of A-TEH to direct voltage during the impacting process. The obtained typical rectified voltage signals under different applied forces are shown in Fig. 6c, which exhibit the same increasing trend with unrectified voltage signals. Such rectified electric energy can continuously and stably charge the capacitor, as demonstrated in Fig. 6d. The ascending charging curves with time well monitored the voltage across the capacitor during the charging process. All of them showed a good linear fitting characteristic during 200 s, and the obtained slopes were summarized in Fig. 6e, which shows the charging rates of A-TEH triggered by different applied impact forces. With the increase of impact forces, the charging capacity of A-TEH was enhanced steadily, from 6.7 mV s^{-1} at 100 N to 11.3 mV s^{-1} at

1400 N. This increasing trend well coincides with the relationships of calculated output power with applied impact force above. We can also use the stored electric power to drive consumer electronics, such as propeller (Fig. 6f) and buzzer alarm (Fig. 6g).

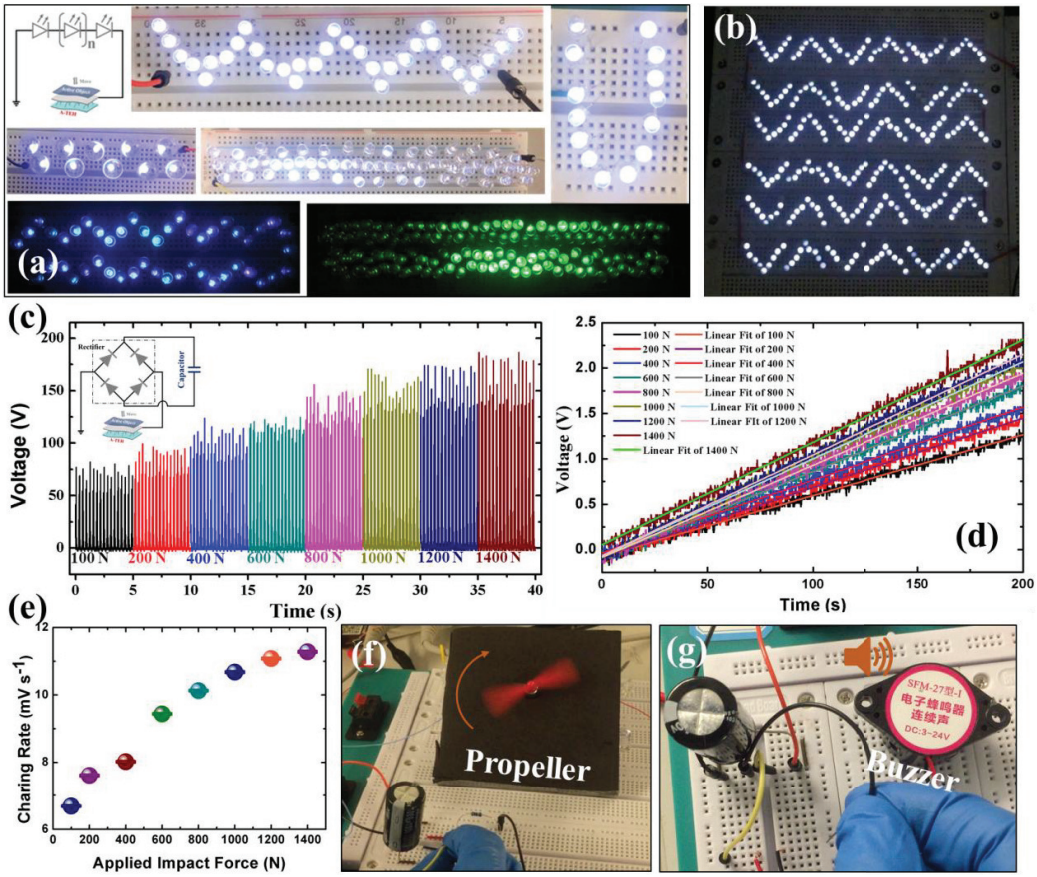

Figure 6 Electric performance of A-TEHs for powering diversified electronics: (a) and (b) different LED arrays directly powered by A-TEHs, (c) rectified output voltages, (d) voltage-time curves of a capacitor charged by A-TEHs and (e) their charging rates, A-TEHs charged a capacitor storage device for powering (f) propeller and (g) buzzer alarm. The insets of (a) and (c) are circuit diagrams of A-TEHs used to drive LEDs directly and charge capacitor after rectification, respectively

Besides full flexibility and high durability, our A-TEHs with excellent electric performance also realize truly safe, comfort and easy-care properties of energy harvesters, including safe fiber materials adopted, good thermal comfort (8.35×10^{-2}

w m^{-1} k^{-1}, higher than 3.00~5.00 x 10^{-2} w m^{-1} k^{-1} of common cotton fabrics), high air-permeability (0.834 kPa s m^{-1}, similar to 1.00~1.20 kPa s m^{-1} of common cotton fabrics), and washability. One of the promising applications of A-TEHs is to be designed and constructed into desired energy devices for harvesting the mechanical energies generated but wasted by human walking in daily life, such as energy harvesting carpets. As demonstrated in Fig. 7a-c, A-TEHs can be directly applied as energy harvesting carpets for electricity generation by harvesting human walking-triggered mechanical energies at different frequency on the floor manufactured with different materials (such as polysiloxane and PVC) or polished with wax. When A-TEH got dirty and resulted in performance degradation, it can be scrubbed with commercial detergent in tap water like common clothes (Fig. 7d, and Movie S5). And their capacity for electric power generation can be recovered again after simply rinsing and drying in air (Fig. 7e). The washability of A-TEH was also conducted on on a vertical-axis washing machine (Whirlpool, USA) referring to AATCC standard 135: dimensional changes of fabrics after home laundering. No visible dimensional (length and width) changes of A-THE sample was observed after machine washing and drying tests (Fig. S4a). And optical microscopic observation at different magnifications further reveals no ruptures found on the washed sample (Fig. S4b and c), suggesting the good fiber structural integrity of A-TEHs. Therefore, the presence of water with detergent and mechanical agitation during the washing process do not damage the structural integrity and electric performance of A-TEHs.

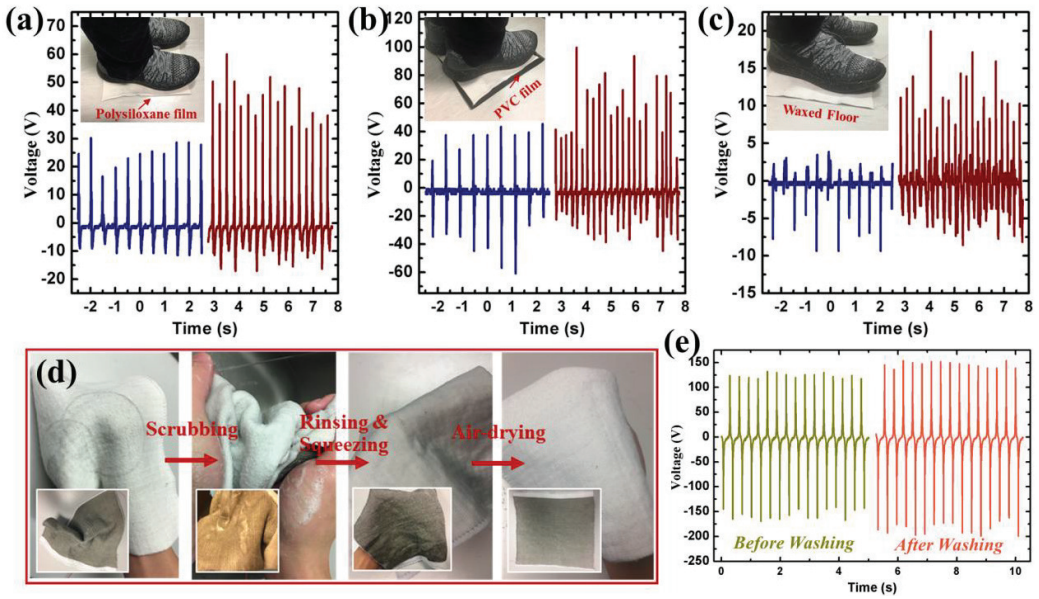

Figure 7 Direct applications of A-TEHs as energy harvesting carpets for harvesting mechanical energies generated by human walking at different frequency on different flooring materials: (a) polysiloxane film, (b) PVC film, and (c) waxed floor, respectively. (d) Photographic process of reactivating A-TEH by washing in water and drying in air. (e) electric performance of A-TEH before and after washing/drying

So far, very less wearable electronics can be directly tailored as required because of the risks on destroying the circuits and electric components. Taking advantages of the unique structural design and single-electrode operation mode, tailorability becomes a unique advantage of our A-TEHs. As shown in Fig. 8a and c, an A-TEH can be directly cut into desired shapes and sizes for direct used as energy harvesters like energy harvesting insole or acting as smart patches to be fully integrated on a common stocking by sewing. The A-TEH insole was inserted into a shoe for generating a peak-to-peak voltage up to 64.2 V by walking (Fig. 8b and inset). And it can be used to harvest the mechanical energy generated by human walking at different frequencies in daily life. The output performance of A-TEH insole generally showed a rise trend with the increase of walking frequency (Fig. S5). For

A-TEH patched stocking, it can be directly put on a foot to harvest the mechanical energies triggered by forefoot (Area I, Fig. 8c) and heel (Area II, Fig. 8c), respectively. As shown in Fig. 8d, approximately 120.0 V can be generated for each A-TEH patch, and when they were connected in series, the generated peak-to-peak voltage can be up to 193.0 V. The electric performance of A-TEHs can be still well maintained during the normal daily activities of the wearer but was found to be slightly decreased after 24 hours, which can be ascribed to the humidity increase of local environment caused by the perspiration of wearer's foot.[39, 40] Nevertheless, benefiting from the robust washability stated above, the electric performance of A-TEHs can be easily recovered *via* normal daily laundry. Movie S6 demonstrates the tailorability of our A-TEHs. These results above show the greatly promising applications of washable and tailorable A-TEH in truly wearable energy harvesting technology.

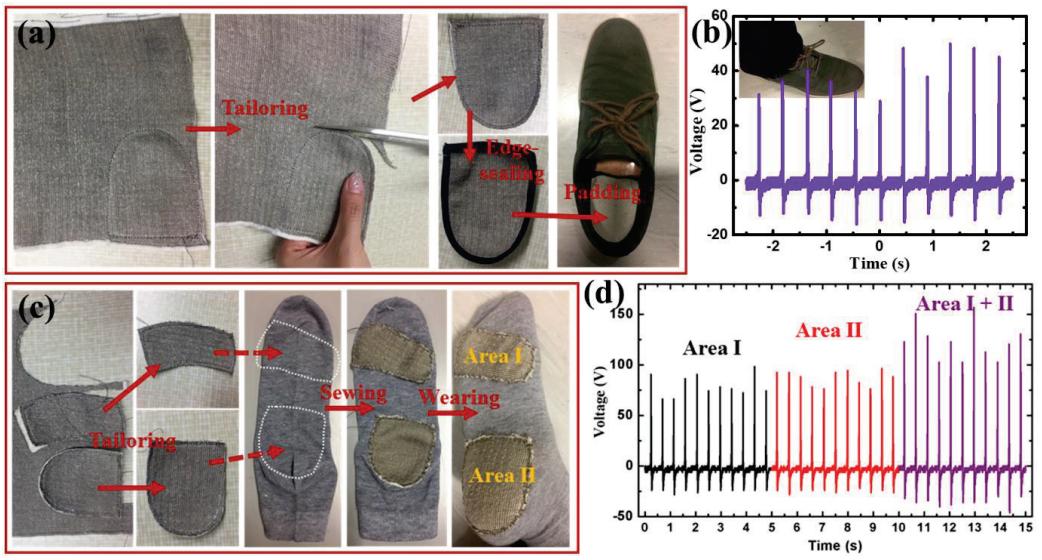

Figure 8 (a) Photographic process of fabricating A-TEH insole by simply cutting and edge-sealing. (b) Electric performance of A-TEH insole triggered by walking. (c) Photographic process of fabricating wearable A-TEH patched stocking by simply cutting and sewing. (d) Electric performances of different A-TEH patches integrated onto the stocking during walking. The inset of (b) shows a A-TEH insole inserted

shoe put on a human foot to harvest mechanical energy by walking

3. Conclusions

In conclusion, we have successfully developed a brand-new kind of A-TEHs with a 3D full fabric structural integrity using only common fiber materials as active components (rather than simply acting as substrate materials) based on a novel mode of energy harvesters by adopting a computerized knitting programme strategy. Benefiting from the novel energy harvesting mode and all fiber structural integrity, our A-TEHs realized the full flexibility of energy harvesters, possessed greatly increased output power, and exhibited stable and durable electric performance. They also introduced the excellent properties of textiles that all wearable electronics try to achieve, including safety, lightweight, comfort, breathability, washability, and unique advantage of tailorability. These properties endowed A-TEHs with truly wearable characteristics and versatile fashion designability to fabricate personal garments and accessories for harvesting mechanical energy generated by human motions. And the adopted textile engineering strategy guaranteed the scalable, rapid and economical fabrication of A-TEHs to act as smart carpets for scavenging the mechanical energies abundantly existed but wasted in the public places. Therefore, this work significantly narrows the gap between high-performed flexible/wearable electronics and truly wearable applications and shows enormous potential applications in the areas of sustainable energy development. It will also open up an avenue to design and fabricate flexible/wearable devices with desired properties and performance for diversified practical applications from the combination of advanced

materials/structures with rich and reliable textile manufacturing techniques.

4. Experimental

4.1 Verification of energy harvesting models

One piece of conductive copper sheet and two pieces of dielectric PDMS films were used for experimental simulation of new energy harvesting mode. One PDMS film was fixed on an upper acrylic plate to act as movable DL-II, while the other PDMS film was fixed on the bottom acrylic plate to act as DL-I. To leave a space between DL-I and DL-II and separate them after compression by external force, four springs were installed at the corners. The copper sheet acting as CL was placed in the middle of two PDMS films with two polyurethane (PU) sponge strips as elastic supports adhered onto the bottom acrylic plate. As a comparison, the copper sheet was directly laminated on DL-I fixed on the bottom acrylic plate to simulate the conventional model without elastic supports. For electric power generation, the upper acrylic plate was repetitively applied with an impacting force to make DL-II to impact CL firstly and then CL to impact DL-I. The triggered process was recorded in real-time by video under a slow-motion mode, and the screenshots during a triggering cycle were captured.

4.2 Direct fabrication of A-TEHs by computerized knitting

The fabrication of A-TEHs was performed on a STOLL computerized flat knitting machine mainly consisted of a carriage and two needle beds positioned horizontally. The carriage that contains computer-aided manufacturing systems carried desired fibers to move across the needle beds back and forth for the fabrication of A-TEHs.

To fabricate a A-TEH, one set of conductive silver-plated nylon fibers and two sets of dielectric polymeric (i.e. cotton and PAN) fibers were used. The fiber size of used conductive silver-plated nylon fibers was 400 denier. And other fiber sizes of cotton and PAN were 340 denier and 600 denier, respectively. The positions of various fibers in the A-TEH structure was controlled by the computerized programme, and its exported schematic was shown in Fig. S3. The fabrication process of A-TEHs can be simply regarded as the repetition of three steps: firstly, the conductive fiber was used to knit the top layer of A-TEH on one needle bed, then PAN fiber was used to knit the bottom layer on the other needle bed, and finally cotton fiber was used to knit middle layer by linking the top layer and bottom layer together.

4.3 Electric performance evaluation of A-TEHs

The electric performance of A-TEHs was evaluated based on a Keyboard Life Tester (ZX-A03) at room temperature of 21.3-21.6 ^{o}C and relative humidity of 53-58%, respectively. The upper plate of tester can provide a continuous dynamic sinusoidal motion with controlled levels of displacement from 0 to 10 mm and frequency from 1 to 5 Hz. During the testing process, a compression force cell was attached to the bottom of energy harvesters for monitoring the applied force. Meanwhile, an oscilloscope with a high voltage probe was connected to A-TEH for monitoring the electric signals during the triggering process. The output voltages across a load with an equivalent resistance of 8 MΩ were measured after achieving a stable value to study the influential factors of triggering forces, triggering frequency and impacting areas. To investigate the influence of external load on the electric performance of

A-TEHs, the triggering force was fixed at 1200 N. The output voltage, current density and power density were determined experimentally. To evaluate the electric performance of A-TEHs for charging energy storage device, a capacitor of 200 μF was connected to a A-TEH with a full bridge rectifier. The rectified voltage and charging curves were determined under different triggering conditions.

4.4 **Characterization**

The microstructures of A-TEHs were characterized by Leica M165C (DFC 290HD, Leica Microsystems Ltd.). And their thickness was measured by a thickness testing instrument (Hans Baer AG, CH-Zurich telex 57767). The thermal conductivity test was conducted on a KES-F7 Thermo Labo II thermal prosperity measurement instrument (Kato Tech. Co., Ltd.) at ambient conditions of approximately 21 ^{o}C and 65% RH. The air permeability was performed by measuring the air resistance of a constant air flow through the A-TEH from and into the atmosphere using an automatic air-permeability tester (KES-F8-AP1, Kato Tech Co., LTD.). The washability test of A-TEH was performed by hand scrubbing with a commercial nonionic detergent in tap water like common garments firstly, then rinsing with water to completely remove residual detergent, and finally wringing water out for air drying. The machine washability test of A-TEHs was conducted on a vertical-axis washing machine (Whirlpool, USA) referring to AATCC standard 135: dimensional changes of fabrics after home laundering. A-TEHs in a mesh bag together with ballast (total load: 1.8 kg) were washed using a commercial nonionic detergent (Castle super concentrate with double lemon fragrance, 66 g) at approximately 40 ^{o}C water at an agitation speed

of 179 - 119 strokes per minute and a spin speed of 645 revolutions per minute for 40 minutes. And they were then dried at 70 ^{o}C for 60 minutes with 'automatic dry' cycle. The durability test of A-TEHs was conducted on a Keyboard Life Tester (ZX-A03) under a constant impacting force of 1200 N. During the testing process, the electric performance of A-TEHs was monitored and determined by an oscilloscope (Keisight DSO-X3014A) with a high voltage probe (Keisight N2790A) under different external loads.

References

[1] S. H. Wang, J. Xu, W. C. Wang, G. J. N. Wang, R. Rastak, F. Molina-Lopez, J. W. Chung, S. M. Niu, V. R. Feig, J. Lopez, T. Lei, S. K. Kwon, Y. Kim, A. M. Foudeh, A. Ehrlich, A. Gasperini, Y. Yun, B. Murmann, J. B. H. Tok, Z. A. Bao, *Nature* **2018**, *555*, 83.

[2] T. Someya, Z. Bao, G. G. Malliaras, *Nature* **2016**, *540*, 379.

[3] J. Y. Oh, S. Rondeau-Gagne, Y. C. Chiu, A. Chortos, F. Lissel, G. N. Wang, B. C. Schroeder, T. Kurosawa, J. Lopez, T. Katsumata, J. Xu, C. Zhu, X. Gu, W. G. Bae, Y. Kim, L. Jin, J. W. Chung, J. B. Tok, Z. Bao, *Nature* **2016**, *539*, 411.

[4] W. Gao, S. Emaminejad, H. Y. Y. Nyein, S. Challa, K. Chen, A. Peck, H. M. Fahad, H. Ota, H. Shiraki, D. Kiriya, D. H. Lien, G. A. Brooks, R. W. Davis, A. Javey, *Nature* **2016**, *529*, 509.

[5] P.-C. Hsu, C. Liu, A. Y. Song, Z. Zhang, Y. Peng, J. Xie, K. Liu, C.-L. Wu, P. B. Catrysse, L. L. Cai, S. Zhai, A. Majumdar, S. H. Fan, Y. Cui, *Sci. Adv*. **2017**, *3*, 8.

[6] P.-C. Hsu, A. Y. Song, P. B. Catrysse, C. Liu, Y. C. Peng, J. Xie, S. H. Fan, Y.

Cui, *Science* **2016**, *353*, 1019.

[7] S. H. Kim, C. S. Haines, N. Li, K. J. Kim, T. J. Mun, C. Choi, J. T. Di, Y. J. Oh, J. P. Oviedo, J. Bykova, S. L. Fang, N. Jiang, Z. F. Liu, R. Wang, P. Kumar, R. Qiao, S. Priya, K. Cho, M. Kim, M. S. Lucas, L. F. Drummy, B. Maruyama, D. Y. Lee, X. Lepro, E. L. Gao, D. Albarq, R. Ovalle-Robles, S. J. Kim, R. H. Baughman, *Science* **2017**, *357*, 773.

[8] N. Soin, T. H. Shah, S. C. Anand, J. F. Geng, W. Pornwannachai, P. Mandal, D. Reid, S. Sharma, R. L. Hadimani, D. V. Bayramol, E. Siores, *Energy Environ. Sci*. **2014**, *7*, 1670.

[9] L. S. Zhang, S. P. Lin, T. Hua, B. L. Huang, S. R. Liu, X. M. Tao, *Adv. Energy Mater.* **2018**, *8*, 1700524.

[10] H. Jinno, K. Fukuda, X. Xu, S. Park, Y. Suzuki, M. Koizumi, T. Yokota, I. Osaka, K. Takimiya, T. Someya, *Nat. Energy* **2017**, *2*, 780.

[11] Y. Meng, Y. Zhao, C. Hu, H. Cheng, Y. Hu, Z. Zhang, G. Shi, L. Qu, *Adv. Mater.* **2013**, *25*, 2326.

[12] H. Sun, Y. Zhang, J. Zhang, X. M. Sun, H. S. Peng, *Nat. Rev. Mater*. **2017**, *2*, 17023.

[13] Z. Z. Zhao, C. Yan, Z. X. Liu, X. L. Fu, L. M. Peng, Y. F. Hu, Z. J. Zheng, *Adv. Mater.* **2016**, *28*, 10267.

[14] W. Zeng, L. Shu, Q. Li, S. Chen, F. Wang, X. M. Tao, *Adv. Mater.* **2014**, *26*, 5310.

[15] M. Gratzel, *Nat. Mater.* **2014**, *13*, 838.

[16] S. J. Kim, J. H. We, B. J. Cho, *Energy Environ. Sci.* **2014**, *7*, 1959.

[17] Y. F. Hu, Z. L. Wang, *Nano Energy* **2015**, *14*, 3.

[18] Z. L. Wang, J. Chen, L. Lin, *Energy Environ. Sci*. **2015**, *8*, 2250.

[19] F. R. Fan, W. Tang, Z. L. Wang, *Adv. Mater.* **2016**, *28*, 4283.

[20] Z. L. Wang, *ACS Nano* **2013**, *7*, 9533.

[21] J. L. Gong, B. G. Xu, X. M. Tao, *ACS Appl. Mater. Interfaces* **2017**, *9*, 4988.

[22] T. C. Hou, Y. Yang, H. Zhang, J. Chen, L. J. Chen, Z. L. Wang, *Nano Energy* **2013**, *2*, 856.

[23] B. Yang, X. Tao, Z. Peng, *Nano Energy* **2019**, *57*, 66.

[24] T. Li, J. Zou, F. Xing, M. Zhang, X. Cao, N. Wang, Z. L. Wang, *ACS Nano* **2017**, *11*, 3950.

[25] S. S. Kwak, H. Kim, W. Seung, J. Kim, R. Hinchet, S.-W. Kim, *ACS Nano* **2017**, *11*, 10733.

[26] T. Zhou, C. Zhang, C. B. Han, F. R. Fan, W. Tang, Z. L. Wang, *ACS Appl. Mater Interfaces* **2014**, *6*, 14695.

[27] M. S. Zhu, Y. Huang, W. S. Ng, J. Y. Liu, Z. F. Wang, Z. Y. Wang, H. Hu, C. Y. Zhi, *Nano Energy* **2016**, *27*, 439.

[28] W. Seung, M. K. Gupta, K. Y. Lee, K. S. Shin, J. H. Lee, T. Y. Kim, S. Kim, J. Lin, J. H. Kim, S. W. Kim, *ACS Nano* **2015**, *9*, 3501.

[29] K. Dong, J. N. Deng, Y. L. Zi, Y. C. Wang, C. Xu, H. Y. Zou, W. B. Ding, Y. J. Dai, B. H. Gu, B. Z. Sun, Z. L. Wang, *Adv. Mater.* **2017**, *29*, 1702648.

[30] K. Dong, Y. C. Wang, J. Deng, Y. Dai, S. L. Zhang, H. Zou, B. Gu, B. Sun, Z. L. Wang, *ACS Nano* **2017**, *11*, 9490.

[31] Z. L. Wang, *Faraday Discuss.* **2014**, *176*, 447.

[32] S. W. Chen, X. Cao, N. Wang, L. Ma, H. R. Zhu, M. Willander, Y. Jie, Z. L. Wang, *Adv. Energy Mater.* **2017**, *7*, 1601255.

[33] H. Guo, T. Li, X. Cao, J. Xiong, Y. Jie, M. Willander, X. Cao, N. Wang, Wang, Z. L. *ACS Nano* 2017, 11, 856.

[34] H. T. Baytekin, A. Z. Patashinski, M. Branicki, B. Baytekin, S. Soh, B. A. Grzybowski, *Science* **2011**, *333*, 308-312.

[35] L. S. McCarty, G. M. Whitesides, *Angew. Chem. Int. Ed.* **2008**, *47*, 2188-2207.

[36] M. M. Apodaca, P. J. Wesson, K. J. M. Bishop, M. A. Ratner, B. A. Grzybowski, *Angew. Chem. Int. Ed.* **2010**, *5*, 946-949.

[37] S. Liu, W. Zheng, B. Yang, X. Tao, *Nano energy* **2018**, *53*, 383.

[38] A. F. Diaz, R. M. Felix-Navarro, *J. Electrostat.* **2004**, *62*, 277.

[39] V. Nguyen, R. Zhu, R. Yang, *Nano Energy* **2015**, *14*, 49.

[40] V. Nguyen, R. Yang, *Nano Energy* **2013**, *2*, 604.